

Analytical solution of the fundamental waveguide mode of 1D transmission grating for TM polarization

A. T. M. Anishur Rahman^{*1}, Krasimir Vasilev² and Peter Majewski¹

¹*School of AME, ²School of AME and Mawson Institute*

University of South Australia

Mawson Lakes, SA 5095, Australia

** Corresponding Author: rahaa001@mymail.unisa.edu.au*

This article presents an analytical solution of the effective index of the fundamental waveguide mode of 1D metallo-dielectric grating for Transverse Magnetic (TM) polarization. In contrast to the existing numerical solution involving transcendental equation, it is shown that the square of the effective index (n_{Eff}) of the fundamental waveguide mode of 1D grating is inversely proportional to the slit width (w) and the refractive index (n_m) of the ridge material and varies linearly with the incident wavelength (λ). Further, it has also been demonstrated that the dependence of n_{Eff} on the grating period (P) and the incidence angle (θ) is minimal. Agreement between the results obtained using the solution presented in this article and published data is excellent. © 2021 Optical Society of America

OCIS codes: 050.0050, 260.1960, 260.2110, 260.3910.

1. Introduction

With the advances in nano and micro fabrication technologies, sub-wavelength structures are now readily achievable [1, 2]. Due to their high brightness in resonance, recently 1D

metallo-dielectric grating structures with sub-wavelength slits ($w < \lambda$, see Fig. 1) have been proposed as useful in flat panel displays, Scanning Near-field Optical Microscopy (SNOM), opto-electronic devices, photo-lithography and tunable optical filter [1–4].

High brightness or resonance in 1D grating can be explained using two different theories [5]. In the regime $\lambda \approx P$, where λ is the wavelength of the incident light and P is the period of the grating, coupling between surface plasmon polariton (SPP) of opposite faces of 1D grating is responsible for enhanced transmission [5], whereas for thick enough grating and $\lambda \gg P$, resonance coupling between a diffraction order and a waveguide mode plays a major role in the extraordinary transmission through 1D metallo-dielectric grating structures [5,6]. In the latter case, depending upon the incident **wavelength**, slit width w and period P , different waveguide modes, both propagating and evanescent, are excited inside the slits [7]. Propagating modes transfer incident energy from one side of the grating to the other and redistribute the transferred energy among the diffraction orders [8]. As the slit width w decreases, more and more modes become evanescent and a very few propagating modes survive [8]. In particular, when w becomes smaller than $\lambda/(2n_d)$, where n_d is the refractive index of the slit/groove, only the fundamental mode propagates and most of the transmitted energy is carried out by this mode [1,2,5,9]. Considering this phenomenon Lalanne et al. have developed an analytical model of transmission through 1D grating for TM polarization [1]. This model can accurately predict resonance wavelengths and their diffraction efficiencies [6]. Finding transmission efficiency using this model requires effective index of the fundamental mode, which is defined as $n_{Eff} = k_z/k_0$, where k_z and k_0 are **the z -component of the wave vector** of the fundamental waveguide mode and **the wave number of the free space** incident electromagnetic illumination respectively [2]. This model also depends on the grating parameters i.e. w , P and h , where h is the thickness of the gratings. Similarly, Porto et al. [5] and Garcia-Vidal et al. [10] have developed models of transmission through 1D gratings by considering only the fundamental mode and their results agree closely with those of Lalanne et al. [1]. Profile of the fundamental mode and x - and z - components of its wave **vector**

(k_x and k_z , see Fig. 1) as well as those of other modes can be determined numerically by solving transcendental modal equation proposed by Sheng et al. in 1982 [7]. This method is known as modal analysis and its solutions, also known as eigenmodes, correspond to various modes of the waveguide structure. Overall this method provides exact description of the modes [8, 11] and is becoming popular [12–15] due to its phenomenological interpretation of the wave propagation via grating structure. Despite this, the method is still a numerical technique and, as inherent to numerical techniques, is devoid of physical insights i.e. can not provide a direct relationship (such as n_{Eff}^2 varies inversely with w) among n_{Eff} , w , P , λ , θ (incidence angle) and n_m (refractive index of the ridge metal) and hence the physics behind the wave propagation via 1D gratings is not well understood. Also, finding a solution of the transcendental equation requires searching inside the variable domains [15] and is computationally demanding [11].

In contrast to the existing numerical solution, in this article we attempt to provide an explicit relation involving n_{Eff} , w , P , n_m , θ and λ . This direct relationship between n_{Eff} and the grating parameters provides a vivid explanation of the physics behind the wave propagation via 1D grating structures. To the best of our knowledge, this kind of analytical model relating n_{Eff} and the grating parameters is nonexistent in the literature for 1D waveguide structures even though such a relationship exists for 2D waveguides [16]. Further, as with analytical solutions, finding n_{Eff} using the method presented here is easy and does not require searching inside the variable domains and consequently it is computationally much less demanding. Also, results obtained using our model agree very closely to those of the exact numerical calculation. In the process of deriving our main result, we assume $w < \lambda/(2n_d)$.

2. Analytical model

Let us consider a TM polarized electromagnetic wave $H_y = \exp(ik_0(\sin \theta x - \cos \theta z)) * \exp(-i\omega t)$ is incident upon the metallo-dielectric grating of Fig. 1 at an incidence angle θ . This incident wave excites various waveguide modes which in turn transfer energy from

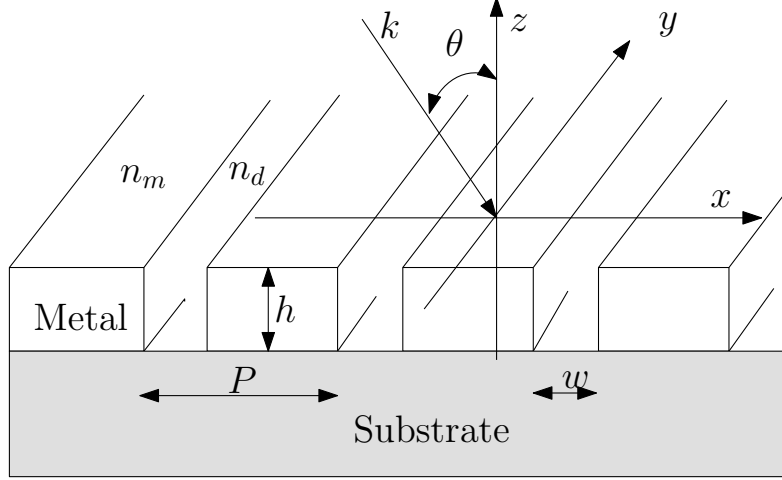


Fig. 1. 1D Lamellar Grating

the incident side ($z > 0$, see Fig. 1) of the grating structure to the outgoing side ($z < -h$). x - and z - components of wave vectors corresponding to different waveguide modes can be obtained by solving transcendental Eq. (1) [7].

$$\cos(k_0 P \sin \theta) - \cos(\beta r P) \cos(\alpha f P) + \frac{1}{2} \left[\frac{\epsilon_m \alpha}{\beta} + \frac{\beta}{\epsilon_m \alpha} \right] \sin(\beta r P) \sin(\alpha f P) = 0 \quad (1)$$

where $\alpha = k_0 \sqrt{\epsilon_d - n_{Eff}^2}$ and $\beta = k_0 \sqrt{\epsilon_m - n_{Eff}^2}$ are the x - components of a waveguide mode in the slit/groove and ridge material respectively. $r = (P - w)/P$, $f = 1 - r = w/P$, $\epsilon_d = n_d^2$ is the dielectric constant of the slit and $\epsilon_m = n_m^2$ is the dielectric constant of the grating ridge. For metallic ridges, dielectric constant is given by $\epsilon_m = n_m^2 = (\eta + i\kappa)^2$, where η and κ are the real and imaginary components of the refractive index. When $|\epsilon_m| \gg |n_{Eff}^2|$, β can be written as $\beta = k_0 n_m$. Assuming $\epsilon_d = n_d^2 = 1$, α can be written as $\alpha = k_0 \rho$, where $\rho = \sqrt{1 - n_{Eff}^2}$. Considering above Eq. (1) can be rewritten as Eq. (2).

$$\cos(k_0 P \sin \theta) - \cos(k_0 n_m r P) \cos(k_0 \rho f P) + \frac{1}{2} \left[\frac{\epsilon_m \alpha}{\beta} + \frac{\beta}{\epsilon_m \alpha} \right] \sin(k_0 n_m r P) \sin(k_0 \rho f P) = 0 \quad (2)$$

Given that $|\epsilon_m| \gg |n_{Eff}^2|$ and $|\epsilon_m \rho^2| \gg 1$, the first factor of the 3rd term of Eq. (2) can be written as $\frac{1}{2} \left[\frac{k_0 \rho \epsilon_m}{k_0 \sqrt{\epsilon_m}} + \frac{k_0 \sqrt{\epsilon_m}}{k_0 \rho \epsilon_m} \right] \approx \sqrt{\epsilon_m} \rho / 2 = n_m \rho / 2$. Based upon this Eq. (2) can be written as Eq. (3).

$$\cos(k_0 P \sin \theta) - \cos q \cos p + \frac{1}{2} n_m \rho \sin q \sin p = 0 \quad (3)$$

where $p = 2\pi \rho w / \lambda$ and $q = 2\pi n_m (P - w) / \lambda$. Expanding $\sin p$ and $\cos p$ into Taylor series, Eq. (3) can be expressed as Eq. (4).

$$\begin{aligned} \frac{1}{2} n_m \rho \left(p - \frac{p^3}{3!} + \frac{p^5}{5!} - \dots \right) \sin q - \left(1 - \frac{p^2}{2!} + \frac{p^4}{4!} - \frac{p^6}{6!} + \dots \right) \cos q + \cos(k_0 P \sin \theta) &= 0 \\ \frac{n_m}{4\pi f \gamma} \left(p^2 - \frac{p^4}{3!} + \frac{p^6}{5!} - \dots \right) \sin q - \left(1 - \frac{p^2}{2!} + \frac{p^4}{4!} - \frac{p^6}{6!} + \dots \right) \cos q + \cos(k_0 P \sin \theta) &= 0 \end{aligned} \quad (4)$$

In the typical operating conditions where only the fundamental mode survives such as ($r = 0.8571$, $f = 0.1429$, $|n_m| \approx 18.73$) [5], ($0.90 \leq r \leq 0.9889$, $0.0111 \leq f \leq 0.10$, $|n_m| \approx 6.796$) [2] and ($0.50 \leq r \leq 0.95$, $0.05 \leq f \leq 0.50$, $|n_m| \approx 5.03$) [15], $|q|$ becomes greater than 1 and $|p|$ is less than unity. In this case any power of p above 4 in Eq. (4) can be neglected. After some simple algebraic manipulations, one can write Eq. (4) as Eq. (5).

$$Ap^4 - Bp^2 + C = 0 \quad (5)$$

where $A = \left(\frac{n_m}{\pi f \gamma} \frac{\sin q}{4!} + \frac{\cos q}{4!} \right)$, $B = \left(\frac{n_m}{2\pi f \gamma} \frac{\sin q}{2!} + \frac{\cos q}{2!} \right)$, $C = (\cos q - \cos(k_0 P \sin \theta))$. Eq. (5) can

be easily solved using the standard algebra and the solutions are given in Eq. (6).

$$\begin{aligned}
p^2 &= \frac{B \pm \sqrt{B^2 - 4AC}}{2A} \\
n_{Eff}^2 &= 1 - \frac{3\lambda^2}{4\pi^2 w^2} \left[1 + \frac{1}{D} \pm \sqrt{1 - \left[\frac{2 \cos q - 8 \cos(k_0 P \sin \theta)}{3 \cos q} \right] \frac{1}{D} + \frac{1}{D^2}} \right] \quad (6)
\end{aligned}$$

where $D = 1 + \frac{\lambda n_m \sin q}{\pi w \cos q}$. $\sin q$ and $\cos q$ can be expanded as $\sin \{k_0(P-w)\eta\} * \cosh \{k_0(P-w)\kappa\} + i \cos \{k_0(P-w)\eta\} \sinh \{k_0(P-w)\kappa\}$ and $\cos \{k_0(P-w)\eta\} * \cosh \{k_0(P-w)\kappa\} - i \sin \{k_0(P-w)\eta\} \sinh \{k_0(P-w)\kappa\}$ respectively. For $k_0(P-w)\kappa > 1$, $\cosh \{k_0(P-w)\kappa\} \approx \sinh \{k_0(P-w)\kappa\}$. In this case, $\sin q$ and $\cos q$ can be written as $\cosh \{k_0(P-w)\kappa\} * \exp[i\{\pi/2 - k_0(P-w)\eta\}]$ and $\cosh \{k_0(P-w)\kappa\} \exp[ik_0(P-w)\eta]$ respectively. After some simple manipulation one can find Eq. (7).

$$\begin{aligned}
n_{Eff}^2 &= 1 - \frac{3\lambda^2}{4\pi^2 w^2} \left[1 + \frac{\pi w}{\pi w + i\lambda n_m} \pm \left[1 - \left[\frac{2}{3} - \frac{8 \cos(k_0 P \sin \theta) \exp \{ik_0(P-w)\eta\}}{3 \cosh \{k_0(P-w)\kappa\}} \right] \right. \right. \\
&\quad \left. \left. \frac{\pi w}{\pi w + i\lambda n_m} + \frac{\pi^2 w^2}{(\pi w + i\lambda n_m)^2} \right]^{1/2} \right] \quad (7)
\end{aligned}$$

Given that $\cosh \{k_0(P-w)\kappa\} \gg 1$ and $|\frac{\pi w}{\pi w + i\lambda n_m}| < 1$, the term under the square root in Eq. (7) can be expanded into binomial series. Neglecting terms of the expansion with power two or more, Eq. (7) can be expressed as Eq. (8).

$$\begin{aligned}
n_{Eff}^2 &= 1 - \frac{3\lambda^2}{4\pi^2 w^2} \left[1 + \frac{\pi w}{\pi w + i\lambda n_m} \pm \left[1 - \left[\frac{1}{3} - \frac{4 \cos(k_0 P \sin \theta) \exp \{ik_0(P-w)\eta\}}{3 \cosh \{k_0(P-w)\kappa\}} \right] \right. \right. \\
&\quad \left. \left. \frac{\pi w}{\pi w + i\lambda n_m} + \frac{\pi^2 w^2}{2(\pi w + i\lambda n_m)^2} \right] \right] \quad (8)
\end{aligned}$$

Provided that $Re(n_{Eff}) \geq 1$, the solution corresponding to the fundamental mode can be

written as Eq. (9).

$$\begin{aligned}
n_{Eff}^2 &= 1 - \left[1 - \frac{\cos(k_0 P \sin \theta) \exp\{ik_0(P-w)\eta\}}{\cosh\{k_0(P-w)\kappa\}} \right] \frac{\lambda^2}{\pi w(\pi w + i\lambda n_m)} + \frac{3\lambda^2}{8(\pi w + i\lambda n_m)^2} \\
&= 1 + i \left[1 - \frac{\cos(k_0 P \sin \theta) \exp\{ik_0(P-w)\eta\}}{\cosh\{k_0(P-w)\kappa\}} \right] \frac{\lambda}{\pi n_m w (1 - i \frac{\pi w}{\lambda n_m})} - \frac{3}{8n_m^2 (1 - i \frac{\pi w}{\lambda n_m})^2} \quad (9)
\end{aligned}$$

Considering $0 < |\frac{i\pi w}{\lambda n_m}| < 1$ and expanding the denominators of the 2^{nd} and 3^{rd} terms of Eq. (9) into binomial series of $\frac{i\pi w}{\lambda n_m}$ and keeping only the first and second power of w and n_m of the expansion respectively, one can represent Eq. (9) as Eq. (10).

$$n_{Eff}^2 = 1 - \left[\frac{11}{8n_m^2} - i \frac{\lambda}{\pi w n_m} \right] + \left[\frac{1}{n_m^2} - i \frac{\lambda}{\pi w n_m} \right] \frac{\cos(k_0 P \sin \theta)}{\cosh\{k_0(P-w)\kappa\}} \exp\{ik_0(P-w)\eta\} \quad (10)$$

3. Results and discussions

The real component of n_{Eff} corresponding to the fundamental mode obtained from Eq. (10) is plotted in Fig. 2 for $n_d = 1$, $\theta = 0^\circ$, $P = 900$ nm and $\lambda = 1433$ nm for silver grating as a function of slit width w . Grating parameters used in this example have been taken from Astilean et al. [2], where the authors show how the effective index of the fundamental mode evolves as the slit width of the grating changes. For the purpose of comparison $Re(n_{Eff})$ from Ref. [2] has also been included in Fig. 2. One can see that there is an excellent agreement between our results and those from Ref. [2]. It is also evident that as w increases, $Re(n_{Eff})$ decreases or there is an inverse relationship between $Re(n_{Eff})$ and w . To confirm this let us look more closely at Eq. (10). Upon consideration one can find that the contribution from the 3^{rd} term in Eq. (10) toward n_{Eff}^2 and hence toward $Re(n_{Eff})$ is very negligible since $\cosh\{k_0(P-w)\kappa\} \gg 1$, $|\exp\{ik_0(P-w)\eta\}| \leq 1$ and $|\cos(k_0 P \sin \theta)| \leq 1$. Considering this one can rewrite Eq. (10) as Eq. (11) from which it is understandable that for fixed P , n_m , λ and θ , n_{Eff}^2 and therefore n_{Eff} vary inversely with w . At this point we quickly mention that this kind of physical insight is not understandable from the existing numerical solution.

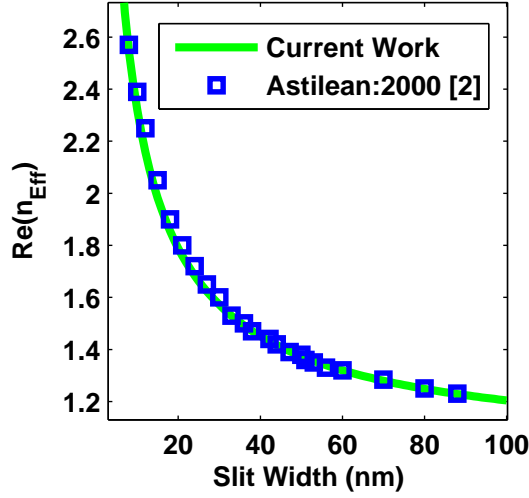


Fig. 2. Real part of the effective index of the fundamental mode as a function of slit width corresponding to $n_d = 1$, $\theta = 0^\circ$, $P = 900$ nm, $\lambda = 1433$ nm for silver gratings

$$n_{Eff}^2 = 1 - \left[\frac{11}{8n_m^2} - i \frac{\lambda}{\pi w n_m} \right] \quad (11)$$

From Eq. (11), one can also find that as $w \rightarrow 0$, n_{Eff}^2 approaches infinity as the grating becomes impermeable to light. On the other hand, when $w \rightarrow \lambda/2$, n_{Eff}^2 approaches a constant value of $1 + \delta$, where $\delta = i \frac{\lambda}{\pi w n_m} - \frac{11}{8n_m^2}$ depends on the dielectric constant of the ridge material and should be much much smaller than unity as $|n_m^2| \gg 1$ has been assumed. When $w = \lambda/2$ and $|n_m^2| \gg 1$ (which is true for most of the metals in the infrared region of the electromagnetic spectrum), $\delta \rightarrow 0$ and n_{Eff}^2 (accordingly n_{Eff}) approaches unity as expected. However, when $0 < w < \lambda/2$ and $|n_m^2| \gg 1$, Eq. (11) can be further simplified to Eq. (12) from which one can observe that n_{Eff}^2 is inversely proportional to w and n_m and varies linearly with λ . For the purpose of demonstration we have plotted data corresponding to Eq. (10) and Eq. (12) in Fig. 3 for the same set of grating parameters of Ref. [2]. It can

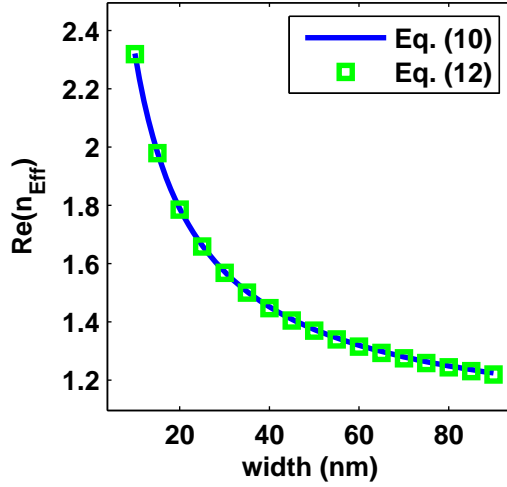


Fig. 3. Real part of the effective index of the fundamental mode as a function of slit width corresponding to $n_d = 1$, $\theta = 0^\circ$, $P = 900$ nm, $\lambda = 1433$ nm for silver gratings

be seen from Fig. 3 that there is no difference between the curves corresponding to Eq. (10) and Eq. (12).

$$n_{Eff}^2 = 1 + i \frac{\lambda}{\pi w n_m} \quad (12)$$

Moreover to verify that n_{Eff}^2 varies inversely with n_m , in Fig. 4 we have plotted both $Re(n_{Eff})$ and $Im(n_{Eff})$ as a function of the refractive index of the ridge material using the exact transcendental Eq. (1) and Eq. (12). This is equivalent to considering various ridge materials while keeping geometrical grating parameters i.e. w , P and h intact. Grating parameters have been taken from [17], where designing 1D grating for extraordinary optical transmission is considered using the numerical optimization technique. From Fig. 4, one can see that there is an excellent agreement between the exact method and the simple analytical method we have presented above. It is also noticeable that as $Im(n_m)$ increases,

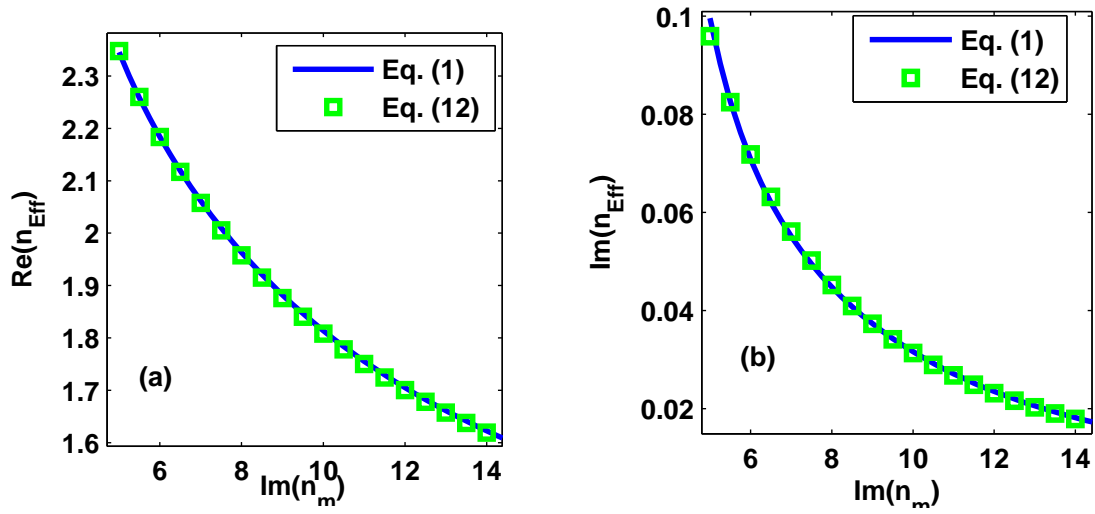


Fig. 4. (a) real and (b) imaginary components of the effective index of the fundamental mode as a function of $Im(n_m)$ while keeping $Re(n_m)$ constant corresponding to $n_d = 1$, $\theta = 0^\circ$, $w = 21$ nm, $P = 150$ nm, $\lambda = 1500$ nm. Grating parameters have been taken from Ref. [17]

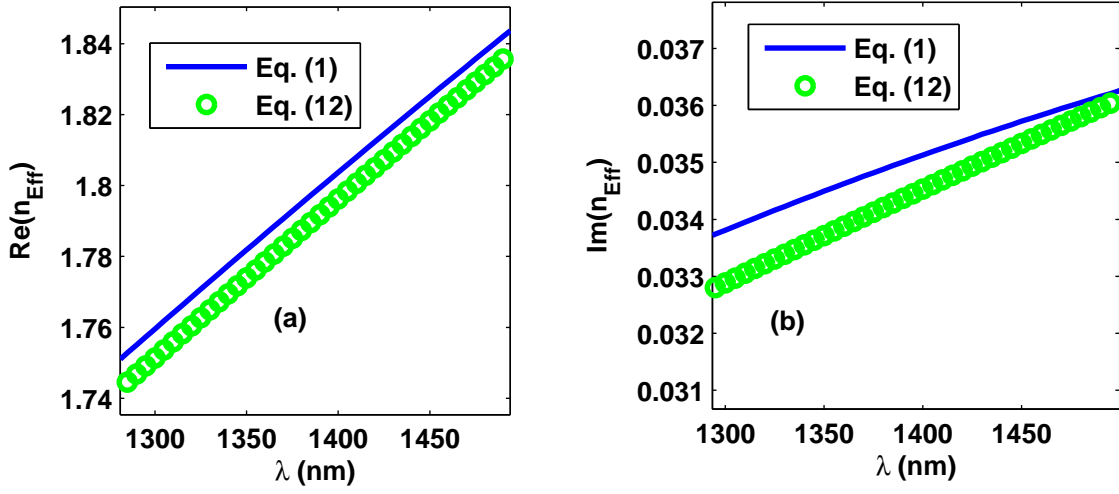


Fig. 5. (a) real and (b) imaginary components of the effective index of the fundamental mode as a function of λ where $n_d = 1$, $\theta = 0^\circ$, $w = 21$ nm and $P = 150$ nm. $n_m = 0.530 + 9.5070i$ is that of gold at $\lambda = 1500$ nm. Grating parameters have been taken from Ref. [17]

loss associated with the fundamental mode ($Im(n_{Eff})$) decreases. This is due to fact that as the imaginary component of the dielectric constant increases, a metal becomes highly reflective and waves can propagate without incurring much loss. Further, although λ and n_m are related, for completeness in Fig. 5 we have plotted both $Re(n_{Eff})$ and $Im(n_{Eff})$ as a function of λ while keeping n_m , w , P and h constant for $\theta = 0^\circ$. The grating geometrical parameters have been taken from Ref. [17] like before and $n_m = 0.530 + 9.5070i$ is that of gold at 1500 nm. Data for this graph have been obtained from the exact numerical calculation (Eq. (1)) and Eq. (12). It can be observed that $Re(n_{Eff})$ and $Im(n_{Eff})$ vary linearly with λ as predicted by Eq. (12) and the agreement between the exact calculation and the simplistic model of n_{Eff} presented in Eq. (12) is very good.

To complete the investigation of the dependence of n_{Eff} on the grating parameters, let us consider the impact of the two remaining parameters, namely the grating period and the

incidence angle on n_{Eff} . According to Eq. (12), n_{Eff}^2 and consequently n_{Eff} do not depend upon these two parameters. However, if one considers Eq. (10), then it is found that the dependence of n_{Eff}^2 on P and θ is very weak. To confirm this we have plotted n_{Eff} as a function of P and θ in Fig. 6 (a) and (b) respectively. In both cases there is a very good qualitative agreement between the exact result obtained by numerically solving Eq. (1) and the calculation performed using Eq. (10). It can be observed that the dependence of n_{Eff} on P and θ is very minimal. In particular, the difference between $Re(n_{Eff})$ corresponding to the two extreme incidence angles ($\theta = 0^\circ$ and $\theta = 90^\circ$) is approximately 0.076%. This is due to the fact that the denominator of the 3rd term of Eq. (10) is much larger than the θ dependent $\cos(k_0 P \sin \theta)$ (varies between -1 and $+1$) in the numerator. Consequently, a relatively small variation in $\cos(k_0 P \sin \theta)$ caused by the variation in θ does not resonate a significant change in n_{Eff} . On the other hand, the dependence of n_{Eff} on P is discernable up to a certain value of the grating period, beyond that it becomes independent of P . This behavior of n_{Eff} in regards to P can be explained by considering Eq. (10) again. For a fixed w , n_m and θ , $\cosh\{k_0(P-w)\kappa\}$ is a real number and is greater than 1. As P and hence $(P-w)$ increases, the denominator of Eq. (10) gets bigger and bigger. When the value of $\cosh\{k_0(P-w)\kappa\}$ is relatively small, the contribution from the 3rd of Eq. (10) towards n_{Eff}^2 is appreciable but when it becomes immensely large, the 3rd term from Eq. (10) can be completely ignored and n_{Eff}^2 becomes independent of P and approaches the value predicted by Eq. (12). In general, it can be concluded that if $2\pi(P-w)\kappa > 10\lambda$ then n_{Eff} does not depend on P significantly. Further, considering the above discussion, one can conclude that the analytical model presented in Eq. (12) for the fundamental mode of 1D grating structure is a very good representation of the exact solution and captures all the physics of the fundamental mode propagation via 1D grating structure. Another interesting point that can be observed from Eq. (12) is that, unlike the 2D structures such as the rectangular waveguides [16], 1D waveguide has no cutoff wavelength above which all modes including the fundamental waveguide mode are non-propagating.

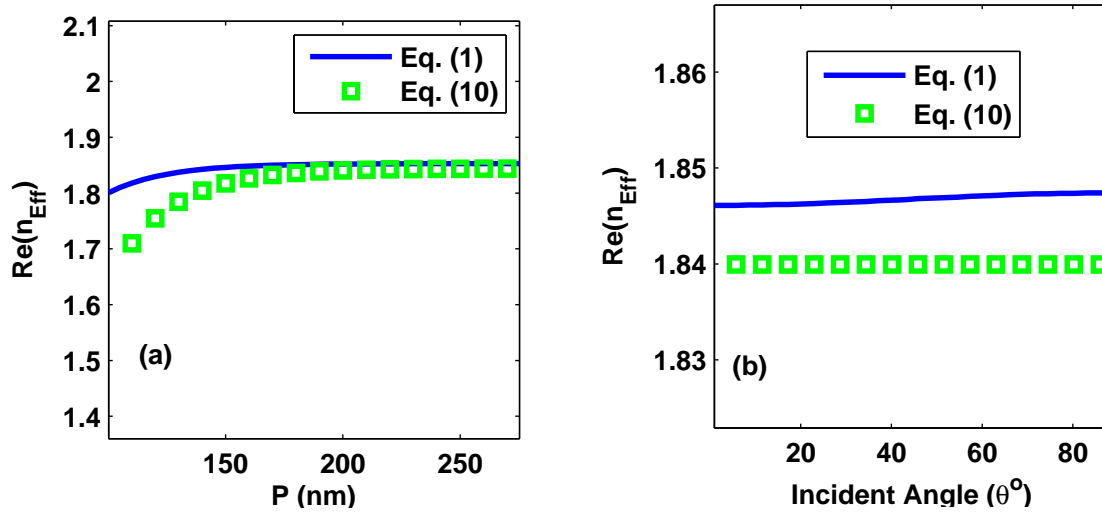


Fig. 6. $Re(n_{Eff})$ as a function of (a) P and (b) incidence angle θ corresponding to $n_d = 1$, $w = 21$ nm and $\lambda = 1500$ nm. For (b) P is equal to 150 nm.

Additionally, to show that the analytical solution of n_{Eff} presented in this article is suitable for different **ridge materials, incidence angles and geometrical grating parameters**, we present more data from the literature and compare them with the data generated using the model presented in Eq. (12). In this regard, we consider data from Ref. [15] where the authors consider aluminum gratings, from Ref. [2] where silver grating is investigated and from Ref. [14] in which loss less metals are considered. Comparative results are presented in Table 1. In all cases, irrespective of ridge materials and incidence angles, the agreement between the current results and those from the literature is good. We present one more example from Ref. [6] where the authors show the negative roles of SPP on EOT for the case of 1D transmission grating for the TM case. In their analysis the authors find the optical transmission of the zeroth diffraction order via 1D grating by using a one-mode (fundamental mode) model of optical transmission [1]. In this model effective index of the fundamental mode is necessary and is determined by the method of line [1]. As per the authors analysis, three different transmission peaks appear at $3.58 \mu\text{m}$, $4.9 \mu\text{m}$ and $9.5 \mu\text{m}$ corresponding to

a gold grating with $w = 0.50 \mu\text{m}$, $h = 4.00 \mu\text{m}$, $P = 3.50 \mu\text{m}$, $n_d = 1$ and $\theta = 0^\circ$. For the purpose of comparison we have plotted the zeroth order transmission efficiency using the same set up of Ref. [6] except n_{Eff} which we have determined using the solution developed in this article (Eq. (12)). From Fig. 7 it can be seen that there are three extraordinary optical transmission peaks at $3.57 \mu\text{m}$, $4.9 \mu\text{m}$ and $9.56 \mu\text{m}$. Upon comparison with the data from Ref. [6], one can find that the agreement between the data generated using our analytical solution and those by calculating n_{Eff} numerically is very good.

Table 1. Effective index corresponding to the fundamental mode with $n_d = 1$.

λ , w and P are given in nm

Grating Parameters	n_{Eff} Literature	n_{Eff} Present Work
Ridge- Silver $\lambda = 1183$, $w = 90$ $P = 900$, $\theta = 0^\circ$	$1.224 + 0.002i$ [2]	$1.220 + 0.002i$
Ridge- Unknown $\lambda = 632.8$, $w = 93.52$ $P = 500$, $\theta = 30^\circ$	1.105 [14]	1.103
Ridge- Aluminum $\lambda = 450$, $w = 100$ $P = 200$, $\theta = 35^\circ$	$1.142 + 0.015i$ [15]	$1.133 + 0.013i$

Finally, we stress that the accuracy of the solution of the fundamental mode presented above significantly depends on the validity of the assumption $|n_{Eff}^2| \ll |\epsilon|$ and whenever this condition is not satisfied there will be a mismatch between the n_{Eff} 's calculated by Eq. (1) and Eq. (12). It is also important to mention that retaining higher powers of p in Eq. (5) does not significantly improve the accuracy of n_{Eff} but increases processing difficulties

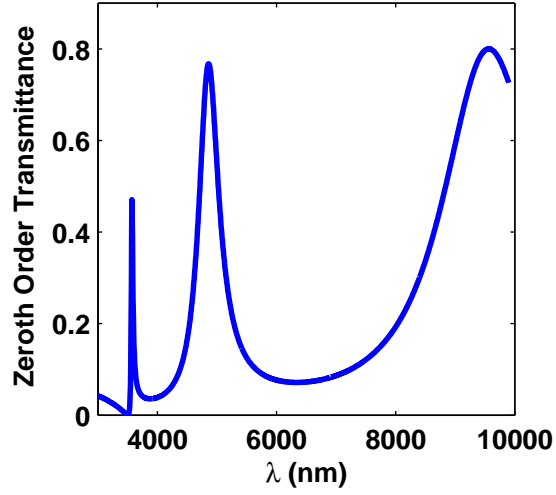


Fig. 7. Zeroth order transmittance corresponding to $P = 3.50 \mu\text{m}$, $w = 0.50 \mu\text{m}$, $h = 4.00 \mu\text{m}$, $n_d = 1$ and $\theta = 0^\circ$ [6]. n_m is that of gold [18]. Transmission efficiency is based on the model of Ref. [1,6] where n_{Eff} is needed to complete the calculation. In Ref. [6] n_{Eff} has been found using a technique called method of line while in plotting this graph we have used Eq. (12)

and overall n_{Eff} becomes an obscure function of w , P , θ , λ and n_m . Lastly, even though we have not considered other grating modes explicitly, conclusions similar to those of the fundamental mode may be applicable to them.

4. Conclusion

In conclusion, we have provided a simple analytical solution of the effective index of the fundamental waveguide mode of 1D grating structure for TM polarization. It has been shown that the square of the effective index of the fundamental waveguide mode is inversely proportional to the slit width and the refractive index of the ridge material. Dependence of n_{Eff} on the grating period and the incidence angle is negligible. The solution provided in this work is very easy to compute and produces results that match closely to those of the exact method. We have also demonstrated that irrespective of the grating materials, incidence angles and incidence wavelength, the analytical solution presented in this article provides reliable results.

References

1. P. Lalanne, J. P. Hugonin, S. Astilean, M. Palamaru, and K. D. Moller, "One-mode model and Airy-like formulae for one-dimensional metallic gratings," *J. Opt. A: Pure Appl. Opt.* **2**, 48-51 (2000).
2. S. Astilean, P. Lalanne, and M. Palamaru, "Light transmission through metallic channels much smaller than the wavelength," *Opt. Commun.* **175**, 265-273 (2000).
3. Y. Pang, C. Genet, and T. Ebbesen, "Optical transmission through subwavelength slit apertures in metallic films," *Opt. Commun.* **280**, 10-15 (2007).
4. T. J. Kim, T. Thio, T. W. Ebbesen, D. E. Grupp, and H. J. Lezec, "Control of optical transmission through metals perforated with subwavelength hole arrays," *Opt. Lett.* **24**, 256-258 (1999).

5. J. A. Porto, F. J. Garcia-Vidal, and J. B. Pendry, "Transmission resonances on metallic gratings with very narrow slits," *Phys. Rev. Lett.* **83**, 2845-2848 (1999).
6. Q. Cao and P. Lalanne, "Negative role of surface plasmons in the transmission of metallic gratings with very narrow slits," *Phys. Rev. Lett.* **88**, 057403 (2002).
7. P. Sheng, R. S. Stepleman, and P. N. Sanda, "Exact eigenfunctions for square-wave gratings: application to diffraction and surface-plasmon calculations," *Phys. Rev. B* **26**, 2907-2916 (1982).
8. A. V. Tishchenko, "Phenomenological representation of deep and high contrast lamellar gratings by means of the modal method," *Opt. Quant. Electron.* **37**, 309-330 (2005).
9. Y. Takakura, "Optical resonance in a narrow slit in a thick metallic screen," *Phys. Rev. Lett.* **86**, 5601-5603 (2001).
10. F. J. García-Vidal and L. Martín-Moreno, "Transmission and focusing of light in one-dimensional periodically nanostructured metal," *Phys. Rev. B* **66**, 155412 (2002).
11. T. Gaylord and M. Moharam, "Analysis and applications of optical diffraction by gratings," in *P. IEEE*, (IEEE, 1985), p. 894-937.
12. T. Clausnitzer, T. Kämpfe, E. B. Kley, A. Tünnermann, U. Peschel, A. V. Tishchenko, and O. Parriaux, "An intelligible explanation of highly-efficient diffraction in deep dielectric rectangular transmission gratings," *Opt. Express* **13**, 10448-10456 (2005).
13. K. R. Catchpole, "A conceptual model of the diffuse transmittance of lamellar diffraction gratings on solar cells," *J. Appl. Phy.* **102**, 013102 (2007).
14. N. M. Lyndin, O. Parriaux, and A. V. Tishchenko, "Modal analysis and suppression of the Fourier modal method instabilities in highly conductive gratings," *J. Opt. Soc. Am. A* **24**, 3781-3788 (2007).
15. M. Foresti, L. Menez, and A. V. Tishchenko, "Modal method in deep metal-dielectric gratings: the decisive role of hidden modes," *J. Opt. Soc. Am. A* **23**, 2501-2509 (2006).
16. R. P. Feynman, R. B. Leighton, and M. Sands, *The Feynman lectures on physics Vol. II*. (Pearson Addison-Wesley, 2006).

17. A. T. M. A. Rahman, K. Vasilev, and P. Majewski, "Designing 1D grating for extraordinary optical transmission for TM polarization," *Photonics Nanostruct.* doc. ID 10.1016/j.photonics.2011.08.002 (posted 17 August, 2011, in press).
18. E. D. Palik, ed., *Handbook of optical constants of solids* (Academic Press, 1985).